Chinese Chemical Letters 31 (2020) 609–616

Contents lists available at ScienceDirect

Chinese Chemical Letters

journal homepage: www.elsevier.com/locate/cclet

Review

Recent advances in metal-organic frameworks for lithium metal anode protection

Ying Du, Xing Gao, Siwu Li, Lu Wang*, Bo Wang*

Beijing Key Laboratory of Photoelectronic/Electrophotonic Conversion Materials, Key Laboratory of Cluster Science, Ministry of Education, School of Chemistry and Chemical Engineering, Beijing Institute of Technology, Beijing 100081, China

ARTICLE INFO

Article history:
Received 18 April 2019
Received in revised form 1 June 2019
Accepted 6 June 2019
Available online 6 June 2019

Keywords:
Metal-organic frameworks
Li anode
Lithium metal batteries
Li dendrite
Protection

ABSTRACT

The lithium metal battery has been considered as a promising candidate for next generation batteries. However, safety concerns caused by uncontrollable lithium dendrite growth on lithium anode are severely hampering the commercial application. Metal-organic frameworks (MOFs) become one of the most attractive materials due to the high porosity, structural designability and tunability. With unique open channels and pores as well as functional components in MOFs, the transportation and deposition of lithium ions can be regulated, which leads to enhanced electrochemical properties. Various strategies for lithium metal protection are proposed in recent works on applications of MOFs in lithium metal batteries. In this review, we highlight latest key approaches in this field and discuss the prospects for MOFs in advanced Li anodes.

© 2019 Chinese Chemical Society and Institute of Materia Medica, Chinese Academy of Medical Sciences. Published by Elsevier B.V. All rights reserved.

1. Introduction

Lithium metal battery (LMB) is considered as one of the most promising batteries for the future energy storage system due to the high theoretical capacity (3860 mA h/g) and lowest redox potential (−3.040 V *vs.* standard hydrogen electrode) of lithium anode [1–4]. However, there remain some challenges greatly hindering its commercial application, such as 1) the safety issue (short circuit and thermal runaway), which could be caused by the uncontrollable Li dendrite growth during the charge process; 2) the increasing internal resistance of batteries due to the accumulative "dead Li" formed on Li anode, significantly decreasing the capacity and lifespan; 3) the unstable and fragile solid electrolyte interphase (SEI) layer on Li metal, consuming lots of electrolytes and fresh Li during the continuous fracture and formation; 4) the volume change in the cycling process, which leads to the drop of native SEI layer from Li metal surface, further destroying the interfacial stability.

Recently, various targeted strategies have been proposed to solve the above-mentioned problems [5–8]. 1) Modification of the current collector [9,10]: coating a lithiophilic material to guide Li nucleation or a robust physical layer to suppress the Li dendrite growth; 2) Construction of anode structure [11–15]: a three-dimensional (3D) Li anode can decrease the volume change and enable dendrite-free Li deposition; 3) Introduction of additives in electrolyte [16,17]: additives can minimize the side reaction and help to obtain a stable SEI layer; 4) Manufacture of artificial SEI [18–23]: artificial SEI layers are more stable than native SEI, which can reduce the consumption of fresh Li and organic electrolyte; 5) Modification of separator [24–27]: the modified separators provide homogeneous channels for Li^+ flux, lead to uniform Li deposition, as well as prevent Li dendrite growth by the mechanical strength; 6) Utilization of solid state electrolytes (SSEs) [28–30]: well-designed SSEs with remarkable chemical stability, high Young's modulus, and superior Li^+ conductivity lead to dendrite-free Li anodes, overcoming security issues of flammable liquid electrolytes.

Metal-organic frameworks (MOFs), a novel class of porous materials constructed by metal nodes and organic linkers, have been widely studied in the field of energy storage and conversion [31–33]. The versatility, porosity, and tunability of MOFs provide effective solutions for LMBs. Recently, various MOFs have been applied to protect Li metal anodes. In this mini review, we mainly focus on the recent progress of MOFs in lithium metal anode protection and summarize applications of MOFs in separators, electrodes and electrolytes for LMBs in detail. The future trends and prospects are also presented here.

2. MOFs in Li metal anode protection

2.1. Solid state electrolytes

Solid-state batteries (SSBs) have attracted much attention because of their unique properties. As is known to all, the liquid

* Corresponding authors.
E-mail addresses: luwang@bit.edu.cn (L. Wang), bowang@bit.edu.cn (B. Wang).

https://doi.org/10.1016/j.cclet.2019.06.013
1001-8417/© 2019 Chinese Chemical Society and Institute of Materia Medica, Chinese Academy of Medical Sciences. Published by Elsevier B.V. All rights reserved.

electrolytes in commercialized Li-ion batteries are suffering from some fatal problems, such as leakage and flammability. Fortunately, the safety issue can be solved by introducing SSEs into SSBs of which Li metal is employed as the anode. However, high interfacial resistance and low ionic conductivity are two major issues of SSBs that inhibit practical application. Therefore, the uppermost priority for high performance SSBs is to develop a solid-state electrolyte with high ionic conductivity, good compatibility with electrodes.

MOFs, the rising star, were first exploited in the field of SSEs by Long's group in 2011 [34]. Mg-MOF-74 based materials with open metal centers exhibit a high ionic conductivity of 3.1×10^{-4} S/cm at room temperature (RT). After that, other MOFs such as ZIF-8 [35], Al-Td-MOF-1 [36], and MIT-20 [37] also have been reported as the ionic conductors. Here, we provide an overview of the recent progress of MOFs as the components in SSEs to protect Li metal anode in SSBs.

2.1.1. Host

Guo and co-authors synthesized a MOF-derived solid-like electrolyte (SLE), in which UiO-66 was used as the host for lithium-containing ionic liquid (Li-IL) owing to the abundant nanopores (Fig. 1a) [38]. In the SLE, MOFs provide stable porous frameworks as the host and the Li-IL acts as the Li^+ conductor. The composite exhibited high ionic conductivity of 3.2×10^{-4} S/cm at 25 °C. However, limited by the low decomposition voltage of Li-IL (4.5 V *vs.* Li/Li^+), this SLE cannot match with the high voltage cathode materials. Chen and co-authors selected ZIF-67 as the host and a stable IL as the guest and prepared a SLE with wide electrochemical window (<5.4 V *vs.* Li/Li^+) [39].

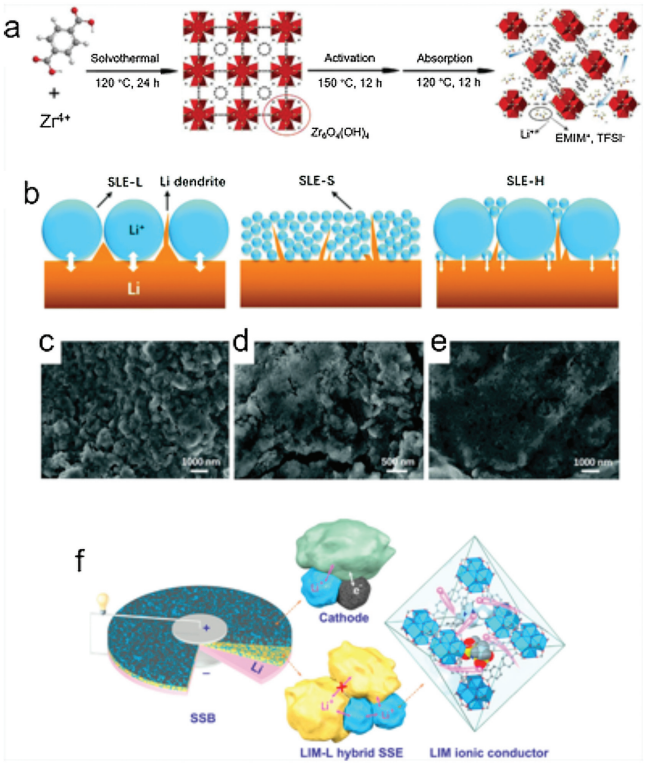

Fig. 1. (a) Preparationprocess of nanostructureUiO/Li-IL SEs. Reprinted with permission [38]. Copyright 2019, Wiley VCH. (b) Schematic illustrations of Li plating/stripping processes at the Li/SLE-L, Li/SLE-S and Li/SLE-H interfaces, respectively. (c-e) SEM morphologies of the Li metal surface after Li plating/stripping cycles of Li|SLE-L|Li, Li|SLE-S|Li and Li|SLE-H|Li symmetric cells, respectively. Reprinted with permission [40]. Copyright 2018, Royal Society of Chemistry. (f) Schematic illustration for the architecture of the SSBs with LIM ionic conductive agent and its working mechanism. The particles with green, yellow, blue, and black color represent the cathode material, LLZO, LIM, and conductive carbon, respectively. $Zr_6(IV)O_4(OH)_4$ clusters in UiO-67 are shown by blue polyhedrons. The migrating Li^+ ions are highlighted by the glowing pink spheres and the $[EMIM]^+$ and $[TFSI]^-$ ions are randomly distributed in the pores of UiO-67 in Space-Filling model. Hydrogen atoms are omitted in the UiO-67 structure for clarity. Reprinted with permission [41]. Copyright 2018, Elsevier.

In Pan's paper, the author prepared three different SLEs: SLE-L, SLE-S, and SLE-H (SLE with large, small, and hybrid size UiO-66 nanoparticles, respectively) to research the size effect on the SSBs performance (Figs. 1c-e) [40]. The SLE-H exhibited the highest ionic conductivity among the others. According to Fig. 1b, the Li metal surface using SLE-H is smoother, which indicates a synergistic effect of the large (suppressing Li dendrite growth) and small (guiding a homogenous Li stripping/plating) nanoparticles of MOFs on SSBs. Pan and co-authors proposed another hybrid SSE by mixing host-guest composites of Li-IL@MOF (UiO-67) with $Li_7La_3Zr_2O_{12}$ (LLZO) to promote the ionic conductivity and block Li dendrite growth (Fig. 1f) [41]. The hybrid SSEs exhibited a wider electrochemical window to 5.2 V, as well as a high ionic conductivity of 1.0×10^{-4} S/cm at room temperature. The interspace between the LLZO grains is fully filled with nano-Li-IL@MOF, which greatly enhances the kinetics of Li^+ transport.

2.1.2. Filler

MOFs impregnated with IL were increasingly utilized in composite polymer electrolytes (CPEs). Pan and co-authors reported a CPE which is consisted of MOFs (MOF-525(Cu)), Li-IL and polytetrafluoroethylene (PTFE) (Fig. 2a) [42]. The composite Li-IL@MOF CPEs exhibited a good thermal stability (over 300 °C) and a stable electrochemical window between 2 V to 4.1 V, as well as a superior electrochemical performance (an ionic conductivity of 3.0×10^{-4} S/cm at room temperature and an enhanced Li^+ transference number of 0.36 compared with 0.14 of pristine Li-IL). The unique nanowetted interfaces between the electrode materials and Li-IL@MOF CPEs enhanced the Li^+ transport kinetics effectively, and the 3D porous nano-structure of MOFs provided an effective Li^+ pathway. On top of that, the SSEs also exhibited a high thermal stability and ionic conductivity within the temperature from −20 °C to 150 °C in the $LiFePO_4$ (LFP) SSBs, performing a capacity of 67 mAh/g in the temperature of −20 °C at 0.05 C and a reversible capacity of 145 mAh/g at 0.5 C in the high temperature of 150 °C (Fig. 2b). PEO solid electrolyte with Li-IL@UiO-66 showed an improved lithium ion conductivity, higher limit voltage and long-term stability.

In 2018, Dunn and co-authors designed a novel class of pseudo solid-state electrolytes using MOFs with open metal sites as the filler to achieve fast Li^+ transport and high ionic conductivity [43]. Sun and co-authors synthesized an anion-immobilized polymer electrolyte using cationic UiO-66 (CMOF) as the filler in poly (ethylene oxide) (PEO) for dendrite-free SSBs [44]. The composite polymer electrolytes can lead to a uniform Li^+ distribution *via* fixing the anions and inhibit the Li dendrite growth by the synergetic effect of PEO with CMOF (Fig. 2c). The ionic conductivity (from 3.9×10^{-6} S/cm to 3.1×10^{-5} S/cm), transference number (as high as 0.72), and electrochemical window (4.97 V) of the CPEs were also significantly improved. Guo and co-authors also reported a PEO-UiO-66/Li-IL CPE that enhanced the SSBs performance [45]. The ionic conductivity of the SPEs greatly increased due to the existence of Li-IL in the porous MOFs structure. More than that, long-lifespan Li|LFP solid-state batteries were performed by introducing UiO-66/Li-IL as the filler for SPEs. Zhang and co-authors reported another Zr-based MOF, NH_2-UiO-66, as the filler for CPEs (Fig. 2d) [46]. The author first proposed a facile photopolymerization with postsynthetic modification MOFs of CPEs with high ionic conductivity (4.31×10^{-4} S/cm at 30 °C) and good interfacial compatibility with electrodes.

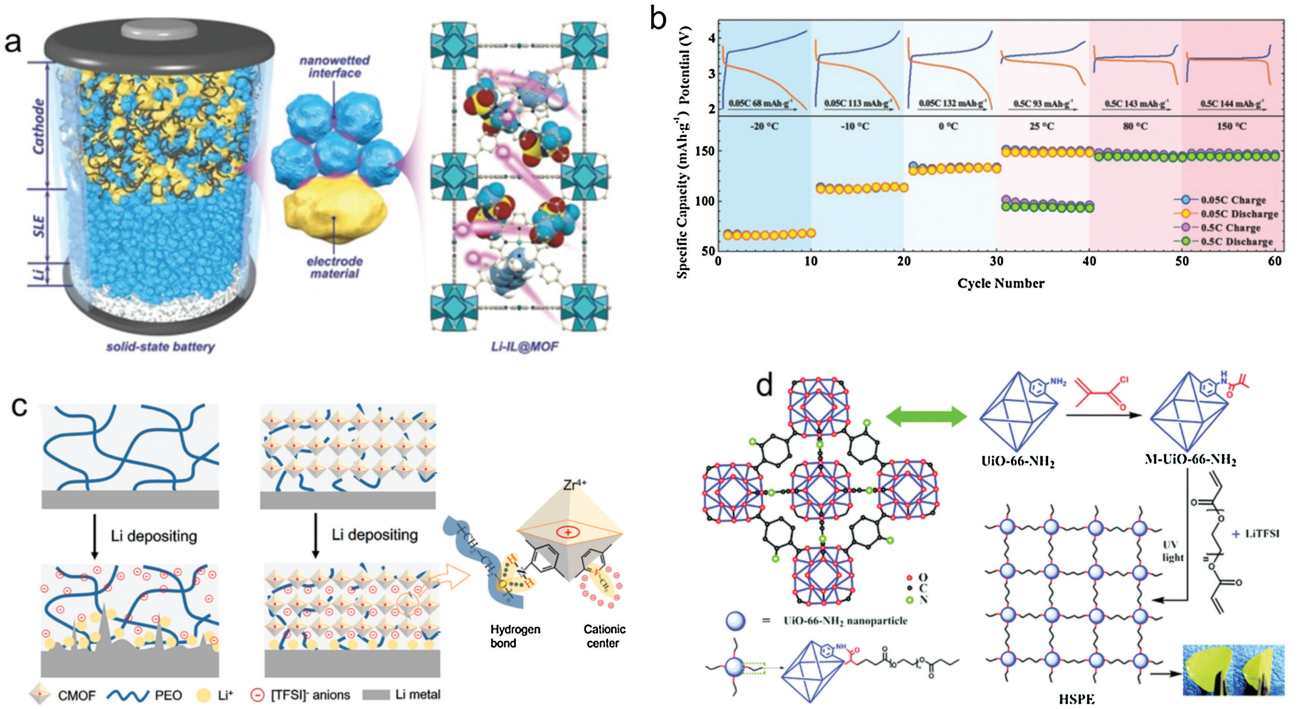

Fig. 2. (a) Schematic illustration for the architecture and nanowetted interfacial mechanism of the solid-state battery with a magnification showing crystal structures of the MOF. $[EMIM]^+$ and $[TFSI]^-$ ions in space-filling model are randomly displayed in the pores of the MOF. The migrating Li^+ ions are highlighted by glowing pink spheres. Hydrogen atoms are omitted in MOF structure for clarity. (b) Temperature-dependent cyclability of the Li|Li-IL@MOF|LFP SSBs with corresponding charge/discharge curves. Reprinted with permission [42]. Copyright 2018, Wiley, VCH. (c) Schematic of the Li deposition behavior with PEO (LiTFSI) electrolyte and anion-immobilized P@CMOF electrolyte. Reprinted with permission [44]. Copyright 2019, Elsevier. (d) Synthetic route of the hybrid covalently linked MOF-PEGDA-based all-solid-state electrolyte. Reprinted with permission [46]. Copyright 2018, Royal Society of Chemistry.

In the above works, whether as host or filler materials for solid electrolytes, MOFs exhibit promising application prospects in high performance SSBs. MOFs with high thermal and chemical stabilities, *e.g.*, Zr-based MOFs, or with special functional groups are good choices for SSEs.

2.2. Separator

Separators, which are indispensable in conventional batteries, provide ion pathway and prevent short circuit. Excitedly, optimizing the separators *via* facile methods can improve the performance of Li metal anodes. Polydopamine coating ameliorates the electrolyte wetting and electrolyte uptake ability of the polyethylene separator, which affect the power performance of batteries directly [47]. The homogeneous pore distribution in the separator leads to a sufficient Li^+ flux and even electrochemical depositions on the electrode surfaces [48]. High ionic conductivity, prominent contact quality and other properties render functional separators potentials to improve the performance of lithium metal batteries.

2.2.1. Coating

The most common method is coating inorganic materials on the commercial separator films, such as Al_2O_3 [49,50], TiO_2 [51,52], and MoS_2 [53]. However, there are some drawbacks that need to be addressed before practical application, including slower Li^+ transport kinetics and deficiency of regulating Li ion redox. In these years, MOFs with inorganic metal ions and organic ligands have been proposed as the modifiers of separators to increase the stability of Li metal anodes.

In Wang's paper, NH_2-MIL-125(Ti) was coated on Celgard 3501, a kind of commercial separators, by doctor blade [54]. After coating, NH_2-MIL-125(Ti) was distributed on the separator uniformly without apparent crack (Figs. 3a–c). The symmetric cell with NH_2-MIL-125(Ti)-coated separators performed a stable cycling for more than 1200 h, whereas the cell with pristine separator displayed a short circuit (Fig. 3d). Further research on the mechanism indicated that the enhanced

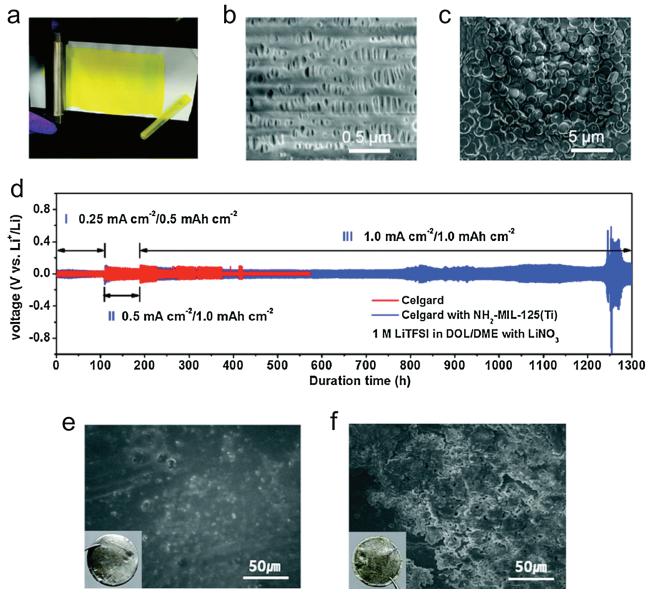

Fig. 3. (a) MOF film coated on PP separator membrane. (b) Top-view SEM image of the pristine separator. (c) Top-view SEM image of the MOF-decorated separator. (d) Voltage profiles of Li metal plating/striping in symmetric Li|Li cells with pristine and NH_2-MIL-125(Ti)-coated separators. Reprinted with permission [54]. Copyright 2017, Royal Society of Chemistry. Digital photographs (inset) and SEM images of the Li metal surface after the cycling process with (e) UiO-66-S/Nafion hybrid-coated separators and (f) the pristine separator. Reprinted with permission [55]. Copyright 2018, Royal Society of Chemistry.

electrochemical performance was benefit from the amine groups on NH_2-MIL-125(Ti), which can greatly promote Li^+ transportation and guide a uniform Li deposition, reducing the possibility of short circuit.

Park and co-authors coated polyethylene (PE) membrane with sulfonated UiO-66 (UiO-66-S) and Nafion, as a functional separator for LMBs [55]. By using the functional separator, the Li metal showed smooth surfaces, whereas Li dendrite (rough particles) on the Li metal surface after cycling was occurred with the pristine separator (Figs. 3e and f). Analogously, the sulfonic acid groups are the keys in inhibiting the polysulfide diffusion and suppressing Li dendrite growth.

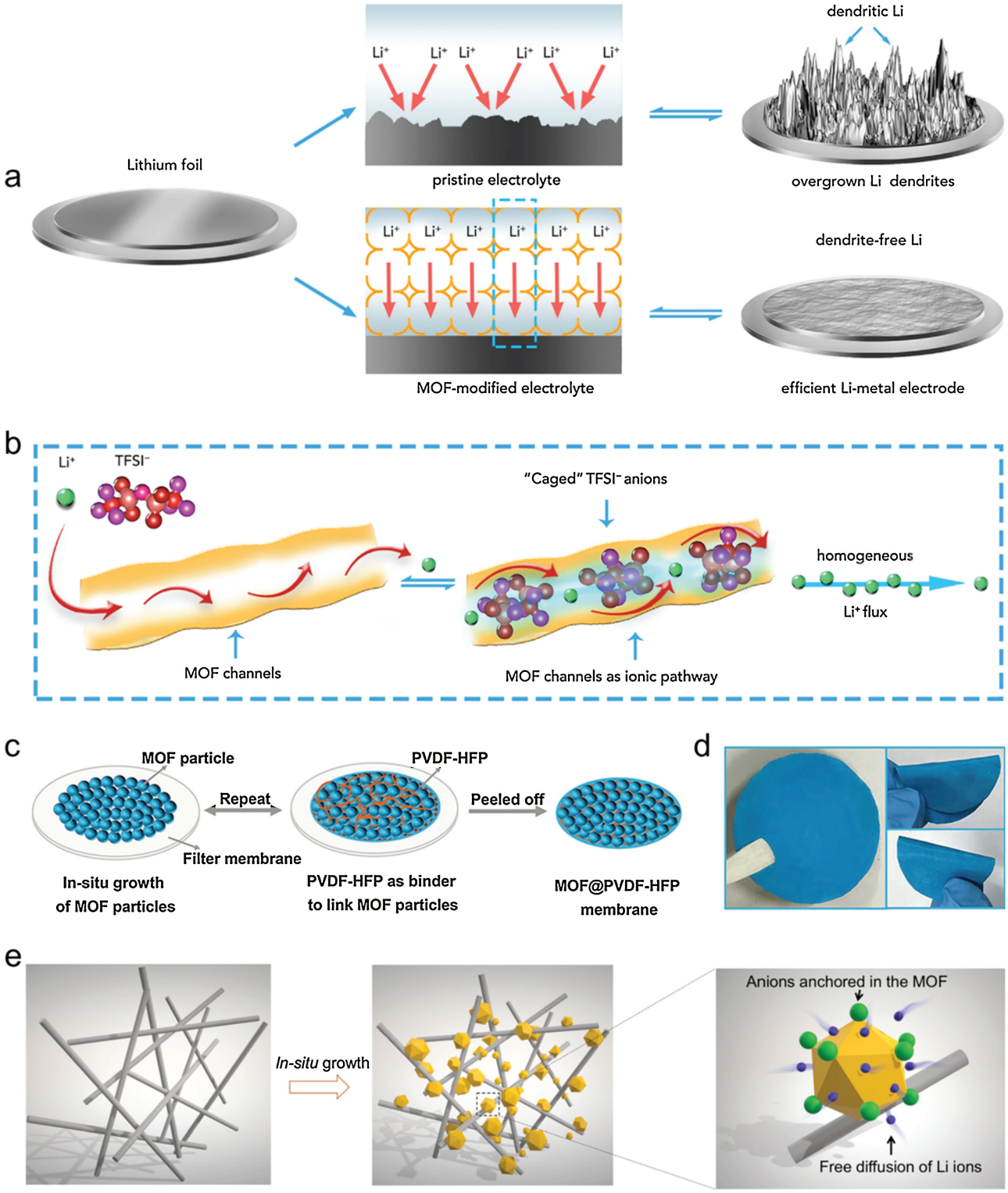

Fig. 4. (a) Schematic showing the Li-metal electrode with pristine electrolyte and MOF-modified electrolyte. (b) Schematic of the selective Li^+ ionic transport imposed by the MOF host. Reprinted with permission [56]. Copyright 2018, Elsevier. (c) Schematic illustration for fabricating a flexible MOF@PVDF-HFP membrane. (d) Digital photos of the flexible MOF@PVDF-HFP separator. Reprinted with permission [57]. Copyright 2018, Wiley VCH. (e) Schematic illustrations of glass fiber (GF), the MOF-GF composite separator (MOG), and an enlarged view showing ion transport behaviours in MOG. Reprinted with permission [58]. Copyright 2019, Royal Society of Chemistry.

As modifiers of separators, MOFs with polar functional groups are proved to be the critical points to obtain long-lifespan batteries with dendrite-free anode. Functionalizing MOFs by amination, carboxylation, hydroxylation and sulfonation is the future trend for utilizing MOFs as the coating in LMBs separators.

2.2.2. Fabricating freestanding separators

Except for ameliorating commercial separator, MOFs can also play an important role in fabricating freestanding separators for LMBs. In 2018, Zhou and co-author proposed a MOF-based separator, which can not only inhibit the polysulfides diffusion but also suppress the dendrite formation benefit from MOFs' porous structure (Figs. 4a and b) [56]. The pore width of HKUST-1 is about 8 Å, and the length of $TFSI^-$ anion (anion of the lithium (bis) trifluoromethanesulfonylimide salt) is 7.9 Å. Considering the size effect, the anions $TFSI^-$ will be restricted within the pores of HKUST-1. However, Li^+ can rapidly transform from the pore channel to the Li metal surface, resulting a homogeneous Li deposition. Zhou and co-authors also reported another HKUST-1-based separator that enhanced the batteries performance (Figs. 4c and d) [57]. In this report, the flexible MOF-based separator, named HKUST-1@PVDF-HFP membrane, was fabricated by filtering HKUST-1 and PVDF-HFP for several times. The membrane not only inhibited the polysulifdes diffusion through physical barrier affection but also guided uniform Li deposition. Owing to these advantages, the Li-S battery with HKUST-1@PVDF-HFP membrane achieved a high initial capacity of 1192 mAh/g, and remained a reversible capacity of 802 mAh/g after 600 cycles. In comparison, the battery with commercial separator remained 304 mAh/g after 600 cycles.

According to above works, we know that the porous structure of MOFs is essential to achieve dendrite-free Li metal anodes. However, besides the effect of pores, the open metal sites of MOFs are also benefit for the enhancement of battery performances. Recently, Lu and co-authors developed a MOF-glass fiber (GF) composite separator (MOG) fabricated by *in situ* growing NH_2-UiO-66 on the GF (Figs. 4e and f) [58]. Li^+ transference number, t_{Li+}, is an indicator for Li^+ transport kinetics in electrolytes, which can be affected by the separator. The t_{Li+} obtained as high as 0.67 after introducing MOG, which is about twice of the pristine GF separator. The high t_{Li+} with MOG led to a smooth and dense Li surface after 100 cycles compared with porous and dendrite surface with bare GF. The enhancements profit from the unsaturated open metal sites with Lewis acidity.

As components of separators in LMBs, MOFs play vital roles in improving the electrochemical performance of batteries. The functional groups, suitable pores/channels and open metal sites, even the particle size of MOFs all benefit the development of advanced LMBs with high energy density.

2.3. Advanced electrodes

The current collector, as a component of the electrodes, affects the performance of Li anode [59]. Li deposition on the conventional current collector usually leads to dendritic growth. Guo *et al.* fabricated a three-dimensional (3D) Cu foil current collector, achieving long-lifespan and dendrite-free lithium metal anode [60].

Li and co-authors designed a MOF modified electrode (Cu-MOFs electrode) to suppress Li dendrite growth (Fig. 5) [61]. Cu-based MOF nanosheets were synthesized to guide well-distributed Li deposition due to the abundant polar functional groups and the high surface area. According to the pioneer works, it has been evidenced that Li nuclei generates immediately when Li^+ obtains e^- on Li metal surface and tends to grow Li dendrite at higher current density. In the MOF modified electrodes, MOFs with high surface area can uptake lots of electrolytes and benefit Li-ions homogeneously flux. After five plating/stripping cycles, top-view SEM images of planar Cu foil showed ununiformed morphology like curved filaments. By contrast, for Cu-MOFs electrodes, uniform cylinder-like Li deposited on the Cu-MOFs layer surface. In the cycling stability test, Cu-MOFs electrode exhibited a considerable

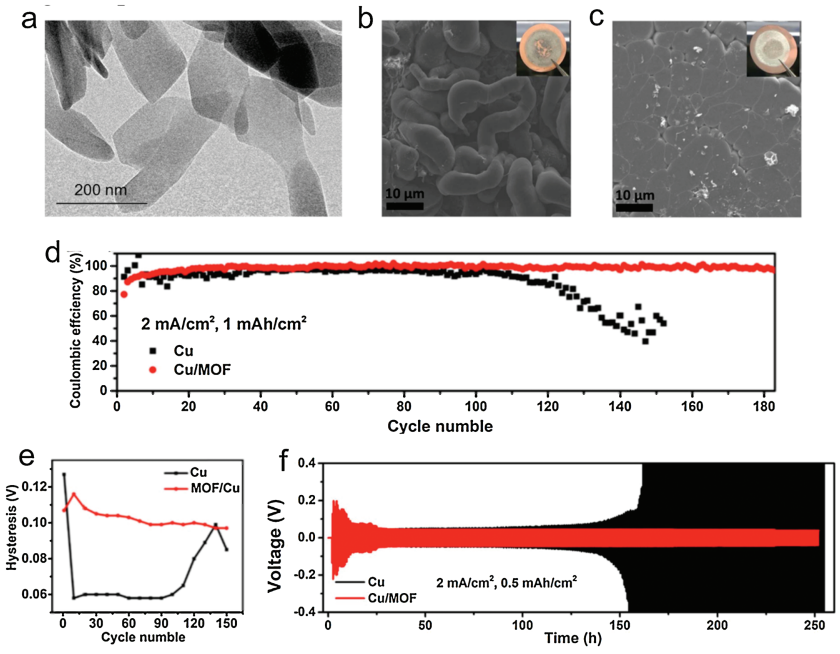

Fig. 5. (a) TEM image of MOF nanosheets. SEM images of surface morphologies of 1.0 mAh/cm^2 Li deposition at a current density of 0.5 mA/cm^2. (b) Bare Cu electrode and (c) Cu-MOFs electrode. The insets are optical images. (d) Comparison of the CE of Li deposition of bare Cu electrode and Cu-MOFs electrode at the current density of 2 mA/cm^2 with a lithiation capacity of 1 mAh/cm^2. (e) Voltage hysteresis of the Li plating/stripping for different electrodes at a current density of 2 mA/cm^2. Symmetrical cell test. (f) The voltage-time curves of 0.5 mAh/cm^2 Li plating/stripping in pre-Li stored Cu electrode and Cu-MOFs electrode symmetrical cell at a current density of 2.0 mA/cm^2. Reprinted with permission [61]. Copyright 2018, Elsevier.

stability, which maintained for more than 180 cycles along with the high Coulombic efficiency (CE) and stable voltage hysteresis. Further evaluation of cycling stability was carried out by assembling symmetric cell to understand the mechanism of interfacial stability. Pre-Li stored Cu-MOF electrode showed consistent voltage plateaus for more than 250 h while the voltage hysteresis of Cu electrode gradually increased to an unacceptable extent.

MOFs, as electrode modifiers integrate the advantages of: 1) high electrolyte absorptivity, 2) polar functional groups, 3) high surface areas, and 4) tunable pore structure. These superiorities may promote MOFs-based electrodes to be widely researched and applied in future.

2.4. Anode structure

Preparing anode with 3D structure is an efficient strategy to control the volume change and restrain Li dendrite [62,63]. However, there are some frameworks lacking lithiophilic sites for Li nucleation, such as carbon fiber network and copper metal foam [64]. Cui and co-authors studied 11 kinds of metal substrate materials and revealed the Li nucleation overpotential on these substrates [65]. It was found that there was no overpotential needed to nucleate lithium on Au, Zn, Mg and Ag, because a solid solution lithium matrix formed before the formation of Li metal. Framework porphyrin (POF) materials were employed as host materials for advanced dendrite-free Li metal anodes because of porphyrin lithiophilic sites [66,67]. The POF-based lithium metal anodes demonstrated superior electrochemical performances, inspiring further investigation of lithiophilic electrochemistry. The results of these reports give a new sight to solve the problems of the unlithiophilic anode structure by introducing nucleation seeds to exactly control the Li deposition and the morphologies of the Li metal surface.

A lithiophilic structure, Ag@MOF, was employed as a lithium host, which is composed of KHUST-1 with abundant oxygen sites and Ag nanoparticals [68]. The Ag@MOF substrate exhibited uniform Li deposition with reduced overpotential.

Yang and co-authors reported a Li-cMOFs (cMOFs: carbonized MOFs) hybrid 3D anode structure greatly inspired by Cui's work, and researched its electrochemical performance (Fig. 6) [69]. ZIF-8, a Zn-based MOF, was chosen in this work. After carbonization, numerous Zn sites are spread on the frameworks universally, and the carbonized ZIF-8 is a lithiophilic host to accommodate the molten Li. During infusion process, Zn can be dissolved into Li, forming a solid soluble layer, and can react with Li to form LiZn alloy, which are the reasons for affinity and low overpotential. In the Li deposition process, the Zn sites in the Li-cMOFs hybrid films can act as nucleation seeds to guide the Li deposition, and the surface of Li-cMOFs film is smooth and dendrite-free. However, after etching the Zn from cMOFs, lithium deposited on the surface of film immediately due to the lack of nucleation sites, forming lithium dendrite on the surface. Similarly, Zhang and co-authors designed a ZnO/carbon/Li advanced anode which provides excellent battery performance [70]. The porous and lithiophilic ZnO/carbon derived from ZIF-8 offers a stable scaffold for Li stripping/plating, mitigates the volume change and dendritic Li growth.

Now there are more than 30, 000 kinds of MOFs with different metal ions or clusters, exhibiting huge potential to obtain carbonized composites which can be employed as templates or precursors. The products, such as metal, metal oxides and metal

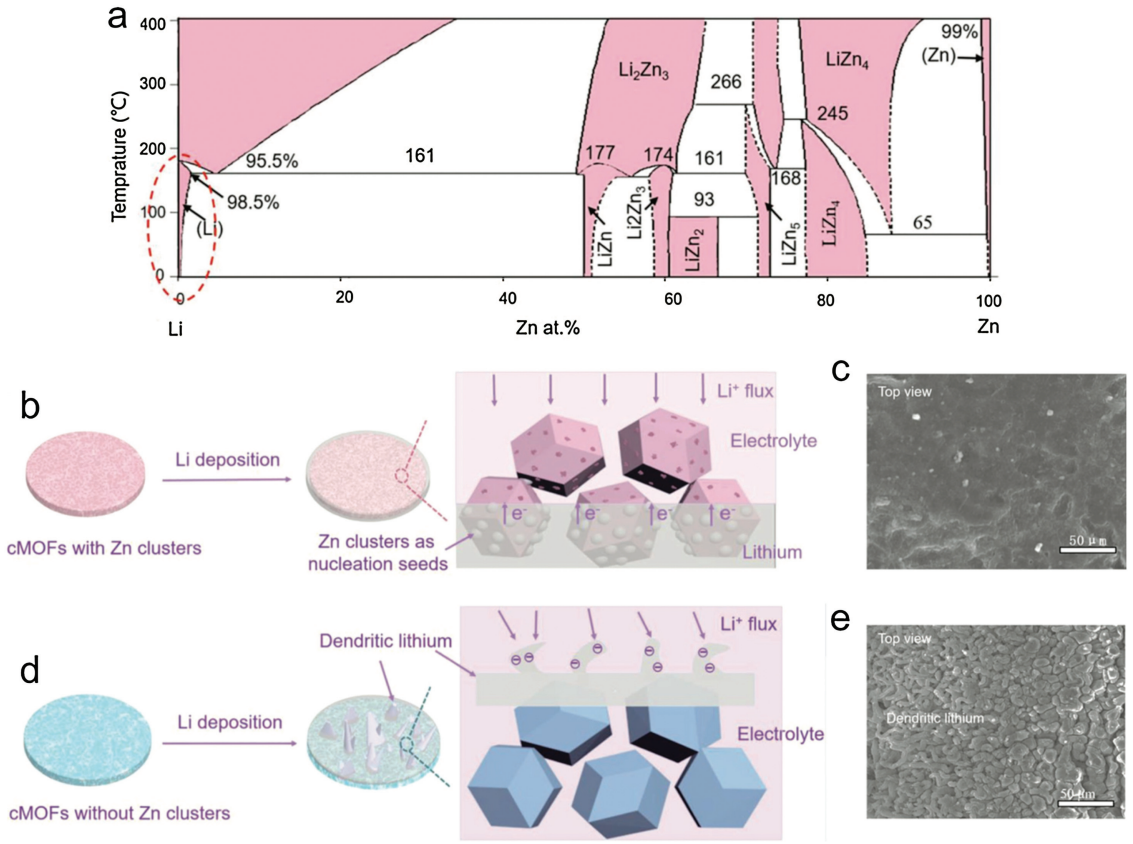

Fig. 6. (a) Phase diagram of Li with Zn. The dashed red circle indicates the solubility of Zn in Li. Li deposition of cMOFs film with and without Zn clusters with capacity of 5 mA h/cm^2. (b) Schematic illustration, and (c) surface SEM images of the Li deposition of the cMOFs film with Zn clusters. (d) Schematic illustration and (e) surface SEM images for the Li deposition of the cMOFs film without Zn clusters. Reprinted with permission [69]. Copyright 2018, Wiley VCH.

sulfides, can act as the lithiophilic sites for Li nucleation and deposition. Besides constructing freestanding Li-cMOFs anodes, we can use other methods like hot-pressing method to introduce MOFs into a network [71,72], forming a lithiophilic 3D anode structure to enhance the electrochemical properties.

2.5. Additives

Improved cycling stability of LMBs can be achieved *via* introducing electrolyte additives [73–77]. In general, the additives will react with Li and form SEI to protect the anodes. In addition, some solid additives have been employed to suppress the Li dendrite [78]. Recently, Li and co-authors proposed three typical MOFs as the electrolyte solid additives to inhibit the Li dendrite growth [79]. In this report, the author synthesized three different MOFs (UiO-66, HKUST-1, NH_2-MIL-101) to discuss the effect of MOFs on Li metal anode. It was found that all MOFs additives stabilized the voltage hysteresis, and UiO-66 exhibited the best cycling performance at the concentration of 1% with lowest overpotential. Compact morphology without dendrites was stabilized by altering Li plating pathway owing to the distinctive structure of MOFs. The UiO-66 additive can suppress the degradation of Li salt anion and other undesired side reactions. Fluorination of UiO-66 also contributed for protecting Li anode from dendrite (Fig. 7).

3. Conclusions and perspectives

Lithium metal has been considered as a "Holy Grail" anode for next generation energy storage batteries since the rechargeable LMBs firstly commercialized in the 1970s. However, the safety problems severely hamper its development. Uncontrollable Li dendrite growth on anode surface during electrodeposition can cause short-circuit and thermal runaway. Besides, "dead Li", side reaction with liquid electrolyte, and volume change are all greatly hindering the practical applications. Various approaches have been proposed to solve the above-mentioned problems in the past decades, such as solid-state electrolytes, 3D anode structure, electrolyte additives, separators, current substrate modification and artificial SEI protection *etc.* MOFs, with the numerous advantages, such as well-defined structure, high surface area, and tunable channels have gained more and more attention in the field of Li anode protection. Overall, we summarized the recent works on utilizing MOFs for high performance LMBs. The main strategies are illustrated schematically in Fig. 8 and summarized below:

1) Solid-state electrolytes: MOFs can act as hosts or fillers in SSEs for solid-state batteries. The stable porous structure of MOFs can provide an efficient Li^+ transport pathway and nanowetted interfaces between electrode materials and MOFs, to enhance the Li^+ transport kinetics and transference number. Introduction of MOFs into SSEs have ameliorated their thermal and electrochemical stabilities, with a wide electrochemical window which usually match with high voltage cathode materials.

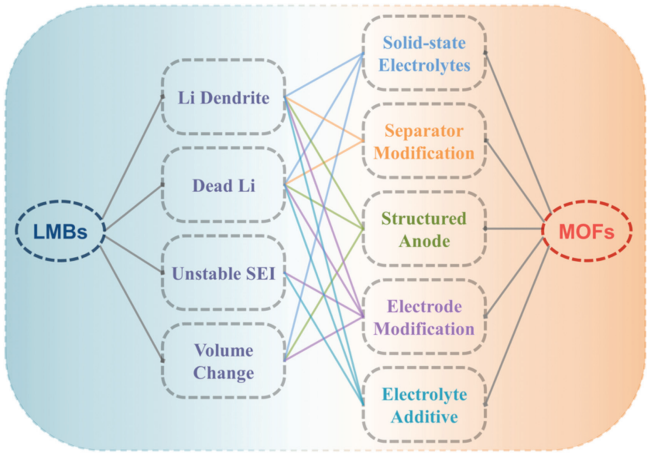

Fig. 8. Selected effective strategies to solve issues of lithium anodes with MOFs for advanced Li metal batteries.

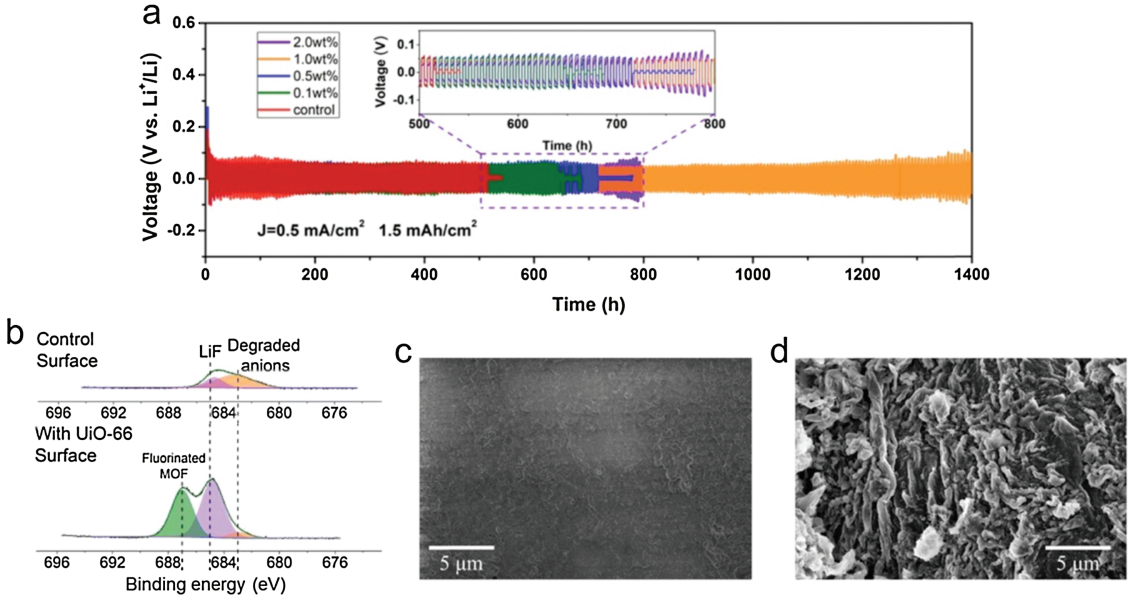

Fig. 7. Li plating/stripping performance of Li|Li symmetric cells based on $LiPF_6$-EC-DMC system containing (a) UiO-66 of different concentrations under a current density of 0.5 mA/cm^2 with a constant areal capacity of 1.5 mAh/cm^2. XPS spectra of (b) F 1s for the cycled Li anode at plating stage for both UiO-66-contained and additive-free $LiPF_6$–EC–DMC systems after five plating/stripping cycles at 0.5 mA/cm^2. SEM images of cycled Li surface morphology at Li plating stage based on Li|Li symmetric cells after 60 cycles at 1 mA/cm^2 with a capacity of 3 mAh/cm^2 for (c) 1 wt% UiO-66-contained and (d) additive-free $LiPF_6$–EC–DMC systems. Reprinted with permission [79]. Copyright 2019, American Chemical Society.

2) Separator modification: MOFs functionalized separators can be prepared *via* i) coating MOFs on a commercialized separator by slurry coating or filtration techniques, and ii) fabricating a freestanding separator using MOFs with graphene oxide or some polymers *etc.* The polar functional groups, open metal sites, and suitable pore channels can promote Li^+ transport kinetics and suppress the Li dendrite growth. Especially the structural particularity of MOFs can restrict anions within the pores and permit Li^+ transmission in the channel. Particle size of MOFs also affects the performance of LMBs.
3) Electrode structure: Constructing 3D Li anode frameworks can effectively control the volume change and the Li dendrite growth during cycling. MOFs and their derivatives provide lithiophilic seeds that can help to diminish the overpotential of Li nucleation and guide uniform Li deposition. In this strategy, MOFs exhibit a huge potential for wide application in LMBs. Modifying current collectors with MOFs is another advisable choice. The MOFs with high surface area can ad/absorb electrolytes within its tunable channels, which is benefit for Li^+ flux.

In a word, MOFs provide various ways to achieve high performance in LMBs. Despite the existing difficulties, we believe that more and more valuable progress will be achieved through precise and targeted design of MOFs for LMBs and the clean energy blueprint will be realized in the near future.

Acknowledgments

This work was financially supported by the National Natural Science Foundation of China (Nos. 21625102, 21471018), the Beijing Municipal Science and Technology Project (No. Z181100004418001), and the Beijing Institute of Technology Research Fund Program.

References

[1] X.B. Cheng, R. Zhang, C.Z. Zhao, et al., Chem. Rev. 117 (2017) 10403–10473.
[2] D.C. Lin, Y.Y. Liu, Y. Cui, Nat. Nanotechnol. 12 (2017) 194–206.
[3] A. Zhamu, G.R. Chen, C.G. Liu, et al., Energy Environ. Sci. 5 (2012) 5701–5707.
[4] Y.P. Guo, H.Q. Li, T.Y. Zhai, Adv. Mater. 29 (2017) 1700007.
[5] J.C. Cui, T.G. Zhan, K.D. Zhang, et al., Chin. Chem. Lett. 28 (2017) 2171–2179.
[6] X. Shen, H. Liu, X.B. Cheng, et al., Energy Storage Mater. 12 (2018) 161–175.
[7] X. Xu, S. Wang, H. Wang, et al., J. Energy Chem. 27 (2018) 513–527.
[8] X.Q. Zhang, C.Z. Zhao, J.Q. Huang, et al., Engineering 4 (2018) 831–847.
[9] X.B. Cheng, T.Z. Hou, R. Zhang, et al., Adv. Mater. 28 (2016) 2888–2895.
[10] Y.M. Liu, X.Y. Qin, S.Q. Zhang, et al., Energy Storage Mater. 18 (2019) 320–327.
[11] Y.Y. Liu, D.C. Lin, Z. Liang, et al., Nat. Commun. 7 (2016) 10992.
[12] T.T. Zuo, X.W. Wu, C.P. Yang, et al., Adv. Mater. 29 (2017) 1700389.
[13] R. Zhang, X. Chen, X. Shen, et al., Joule 2 (2018) 764–777.
[14] Z.W. Sun, S. Jin, H.C. Jin, et al., Adv. Mater. 30 (2018) 1800884.
[15] K. Liu, B. Kong, W. Liu, et al., Joule 2 (2018) 1857–1865.
[16] H. Zhang, G.G. Eshetu, X. Judez, et al., Angew. Chem. Int. Ed. 57 (2018) 15002–15027.
[17] X.Q. Zhang, X.B. Cheng, X. Chen, et al., Adv. Funct. Mater. 27 (2017) 1605989.
[18] N.W. Li, Y.X. Yin, C.P. Yang, et al., Adv. Mater. 28 (2016) 1853–1858.
[19] X. Liang, Q. Pang, I.R. Kochetkov, et al., Nat. Energy 2 (2017) 17119.
[20] J. Lopez, A. Pei, J.Y. Oh, et al., J. Am. Chem. Soc. 140 (2018) 11735–11744.
[21] C. Yan, X.B. Cheng, Y. Tian, et al., Adv. Mater. 30 (2018) 1707629.
[22] Y.X. Yuan, F. Wu, Y. Bai, et al., Energy Storage Mater. 16 (2019) 411–418.
[23] B. Zhu, Y. Jin, X.Z. Hu, et al., Adv. Mater. 29 (2017) 1603755.
[24] S.Y. Bai, K. Zhu, S.C. Wu, et al., J. Mater. Chem. A 4 (2016) 16812–16817.
[25] M.M. Chi, L.Y. Shi, Z.Y. Wang, et al., Nano Energy 28 (2016) 1–11.
[26] H. Lee, X.D. Ren, C.J. Niu, et al., Adv. Funct. Mater. 27 (2017) 1704391.
[27] C.F. Li, S.H. Liu, C.G. Shi, et al., Nat. Commun. 10 (2019) 1363.
[28] R.J. Chen, W.J. Qu, X. Guo, et al., Mater. Horiz. 3 (2016) 487–516.
[29] A. Manthiram, X.W. Yu, S.F. Wang, Nat. Rev. Mater. 2 (2017) 16103.
[30] C.P. Yang, K. Fu, Y. Zhang, et al., Adv. Mater. 29 (2017) 1701169.
[31] J.W. Zhou, B. Wang, Chem. Soc. Rev. 46 (2017) 6927–6945.
[32] H.B. Zhang, J.W. Nai, L. Yu, et al., Joule 1 (2017) 77–107.
[33] R. Zhao, Z.B. Liang, R.Q. Zou, et al., Joule 2 (2018) 2235–2259.
[34] B.M. Wiers, M.L. Foo, N.P. Balsara, et al., J. Am. Chem. Soc. 133 (2011) 14522–14525.
[35] K. Fujie, R. Ikeda, K. Otsubo, et al., Chem. Mater. 27 (2015) 7355–7361.
[36] S. Fischer, J. Roeser, T.C. Lin, et al., Angew. Chem. Int. Ed. 57 (2018) 16683–16687.
[37] S.S. Park, Y. Tulchinsky, M. Dincă, J. Am. Chem. Soc. 139 (2017) 13260–13263.
[38] J.F. Wu, X. Guo, Small 15 (2019) e1804413.
[39] N. Chen, Y. Li, Y. Dai, et al., J. Mater. Chem. A 7 (2019) 9530–9536.
[40] K. Wang, L.Y. Yang, Z.Q. Wang, et al., Chem. Commun. 54 (2018) 13060–13063.
[41] Z.Q. Wang, Z.J. Wang, L.Y. Yang, et al., Nano Energy 49 (2018) 580–587.
[42] Z.Q. Wang, R. Tan, H.B. Wang, et al., Adv. Mater. 30 (2018) 1704436.
[43] L. Shen, H.B. Wu, F. Liu, et al., Adv. Mater. 30 (2018) 1707476.
[44] H.Y. Huo, B. Wu, T. Zhang, et al., Energy Storage Mater. 18 (2019) 59–67.
[45] J.F. Wu, X. Guo, J. Mater. Chem. A 7 (2019) 2653–2659.
[46] Z.N. Wang, S. Wang, A.L. Wang, et al., J. Mater. Chem. A 6 (2018) 17227–17234.
[47] M.H. Ryou, Y.M. Lee, J.K. Park, et al., Adv. Mater. 23 (2011) 3066–3070.
[48] R.J. Pan, X.X. Xu, R. Sun, et al., Small 14 (2018) 1704371.
[49] H.S. Jeong, S.C. Hong, S.Y. Lee, J. Membr. Sci. 364 (2010) 177–182.
[50] Y.P. Guan, A.B. Wang, S. Liu, et al., J. Alloys Compd. 765 (2018) 544–550.
[51] H.Y. Shao, W.K. Wang, H. Zhang, et al., J. Power Sources 378 (2018) 537–545.
[52] X.M. Zhu, X.Y. Jiang, X.P. Ai, et al., J. Membr. Sci. 504 (2016) 97–103.
[53] Z.A. Ghazi, X. He, A.M. Khattak, et al., Adv. Mater. 29 (2017)1606817.
[54] W. Liu, Y.Y. Mi, Z. Weng, et al., Chem. Sci. 8 (2017) 4285–4291.
[55] S.H. Kim, J.S. Yeon, R. Kim, et al., J. Mater. Chem. A 6 (2018) 24971–24978.
[56] S.Y. Bai, Y. Sun, J. Yi, et al., Joule 2 (2018) 2117–2132.
[57] Y.B. He, Z. Chang, S.C. Wu, et al., Adv. Energy Mater. 8 (2018)1802130.
[58] L. Shen, H.B. Wu, F. Liu, et al., Nanoscale Horiz. 4 (2019) 705–711.
[59] Q. Li, S.P. Zhu, Y.Y. Lu, Adv. Funct. Mater. 27 (2017) 1606422.
[60] C.P. Yang, Y.X. Yin, S.F. Zhang, et al., Nat. Commun. 6 (2015) 8058.
[61] Z.G. Jiang, T.F. Liu, L.J. Yan, et al., Energy Storage Mater. 11 (2018) 267–273.
[62] S.S. Chi, Y.C. Liu, W.L. Song, et al., Adv. Funct. Mater. 27 (2017) 1700348.
[63] A.M. Hafez, Y.C. Jiao, J.J. Shi, et al., Adv. Mater. 30 (2018) 1802156.
[64] Z. Liang, D.C. Lin, J. Zhao, et al., Proc. Natl. Acad. Sci. U. S. A. 113 (2016) 2862–2867.
[65] K. Yan, Z.D. Lu, H.W. Lee, et al., Nat. Energy 1 (2016) 16010.
[66] X.R. Chen, B.Q. Li, C.X. Zhao, et al., Small Methods (2019) 1900177.
[67] B.Q. Li, X.R. Chen, X. Chen, et al., Research 2 (2019) 4608940.
[68] S. Yuan, J.L. Bao, C. Li, et al., ACS Appl. Mater. Interfaces 11 (2019) 10616–10623.
[69] M.Q. Zhu, B. Li, S.M. Li, et al., Adv. Energy Mater. 8 (2018) 1703505.
[70] L.Y. Wang, X.Y. Zhu, Y.P. Guan, et al., Energy Storage Mater. 11 (2018) 191–196.
[71] Y.F. Chen, S.Q. Li, X.K. Pei, et al., Angew. Chem. Int. Ed. 55 (2016) 3419–3423.
[72] X. Gao, Y. Du, J.W. Zhou, et al., ACS Appl. Energy Mater. 1 (2018) 6986–6991.
[73] Q.C. Liu, J.J. Xu, S. Yuan, et al., Adv. Mater. 27 (2015) 5241–5247.
[74] G.X. Li, Y. Gao, X. He, et al., Nat. Commun. 8 (2017) 850.
[75] Q. Pang, X. Liang, A. Shyamsunder, et al., Joule 1 (2017) 871–886.
[76] B. Tong, J.W. Wang, Z.J. Liu, et al., J. Power Sources 400 (2018) 225–231.
[77] X. Zhang, Q.M. Zhang, X.G. Wang, et al., Angew. Chem. Int. Ed. 57 (2018) 12814–12818.
[78] L. Chen, J.G. Connell, A. Nie, et al., J. Mater. Chem. A 5 (2017) 12297–12309.
[79] F.L. Chu, J.L. Hu, C.L. Wu, et al., ACS Appl. Mater. Interfaces 11 (2019) 3869–3879.